ANALYSIS AND MATHEMATICAL MODELLING OF SPACE VECTOR MODULATED DIRECT CONTROLLED MATRIX CONVERTER

[1,2]RUZLAINI GHONI, [2]AHMED N. ABDALLA

[1]Faculty of Electrical Automation Engineering Technology, TATiUC, Terengganu, Malaysia-24000

[2]Faculty of Electrical and Electronic Engineering, UMP, Kuantan, Malaysia -26300

ABSTRACT

Matrix converters as induction motor drivers have received considerable attention in recent years because of its good alternative to voltage source inverter pulse width modulation (VSI-PWM) converters. This paper presents the work carried out in developing a mathematical model for a space vector modulated (SVM) direct controlled matrix converter. The mathematical expressions relating the input and output of the three phase matrix converter are implemented by using MATLAB/SIMULINK. The duty cycles of the switches are modeled using space vector modulation for 0.5 and 0.866 voltage transfer ratios. Simulations of the matrix converter loaded by passive *RL* load and active induction motor are performed. A unique feature of the proposed model is that it requires very less computation time and less memory compared to the power circuit realized by using actual switches. In addition, it offers better spectral performances, full control of the input power factor, fully utilization of input voltages, improve modulation performance and output voltage close to sinusoidal.

Keywords: *Matrix Converter, Space Vector Modulation, Simulation Model, Induction Motor*

1. INTRODUCTION

Recently, the induction motor fed from three phase matrix converter has established their importance in industrial drive applications. In reality, the matrix converter provides important benefits such as bidirectional power flow, sinusoidal input current with adjustable displacement angle (i.e. controllable input power factor), and a great potential for size reduction due to the lack of dc-link capacitors for energy storage [1-3].

Various modulation methods for matrix converters have been investigated. Indirect AC-AC modulation [4], PWM patterns for nine switches of the matrix converter are generated directly from the output voltage reference and the input current reference. In virtual AC-DC-AC modulation [5], the matrix converter is controlled as a combination of a virtual current source PWM rectifier and a virtual voltage source PWM inverter, and then switching patterns for the matrix converter are synthesized. In the latter case, the problem is that when switching patterns are generated to obtain a zero voltage vector in the virtual inverter, phase currents do not flow in the virtual rectifier regardless of the switching patterns for the rectifier, and as a result, the input current waveforms become distorted. In [5], this problem was solved by changing the carrier wave on the virtual inverter side. Another solution involves applying space vector modulation to the virtual rectifier inverter control [6-8]. In yet another method, the maximum input line-to-line voltage is discarded in PWM modulation when the modulation factor is low, thus suppressing harmonics in the output voltage [9]. The present study deals with space vector modulation (SVM) in virtual rectifier inverter control within the frame-work of virtual AC-DC-AC modulation [6-8].

In this paper, induction motor fed by direct controlled matrix converter with a space vector modulated (SVM) was proposed. A complete mathematical analysis of the power circuit along with the duty cycle calculation (switching algorithm) is described for both low voltage transfer ratio (0.5) and maximum voltage transfer ratio (0.866). The whole model is then realized by using Simulink blocks such as math operators, relational operators, and delay circuits. Finally, the proposed

mathematical model is validated using a passive *RL* load and active induction motor load.

2. SPACE VECTOR MODULATION

Space Vector Modulation refers to a special switching sequence which is based on the upper switches of a three phase matrix converter. Theoretically, SVM treats a sinusoidal voltage as a phasor or amplitude vector which rotates at a constant angular frequency, ω. This amplitude vector is represented in *d-q* plane where it denotes the real and imaginary axes. As SVM treats all three modulating signals or voltages as one single unit, the vector summation of three modulating signals or voltages are known as the reference voltage, V_{oref} which is related to the magnitude of output voltage of the switching topologies. The aim of SVM is to approximate the reference voltage vector, V_{oref} from the switching topologies.

For a balanced three phase sinusoidal system the instantaneous voltages maybe expressed as (1)

$$\begin{bmatrix} V_u(t) \\ V_v(t) \\ V_w(t) \end{bmatrix} = V_o \begin{bmatrix} \cos \omega_0 t \\ \cos(\omega_0 t - 120^\circ) \\ \cos(\omega_0 t - 240^\circ) \end{bmatrix} \quad (1)$$

This can be analyzed in terms of complex space vector

$$\vec{V}_o = \frac{2}{3}\left[V_u(t) + V_v(t)e^{\frac{j2\pi}{3}} + V_w(t)e^{\frac{j4\pi}{3}}\right] = V_o e^{j\omega_0 t} \quad (2)$$

Where $e^{j\theta} = \cos\theta + j\sin\theta$ and represents a phase shift operator and 2/3 is a scaling factor equal to the ratio between the magnitude of the output line-to-line voltage and that of output voltage vector. The angular velocity of the vector is ω_0 and its magnitudeV_o.

Similarly, the space vector representation of the three phase input voltage is given by (3)

$$\vec{V}_i = \frac{2}{3}\left[V_a(t) + V_b(t)e^{\frac{j2\pi}{3}} + V_c(t)e^{\frac{j4\pi}{3}}\right] = V_i e^{j\omega_i t} \quad (3)$$

Where V_i is the amplitude and ω_i, is the constant input angular velocity.

If a balanced three phase load is connected to the output terminals of the converter, the space vector forms of the three phase output and input currents are given by

$$\vec{I}_o = \frac{2}{3}\left[I_u(t) + I_v(t)e^{\frac{j2\pi}{3}} + I_w(t)e^{\frac{j4\pi}{3}}\right] = I_o e^{j(\omega_0 t - \emptyset_o)} \quad (4)$$

$$\vec{I}_i = \frac{2}{3}\left[I_a(t) + I_b(t)e^{\frac{j2\pi}{3}} + I_c(t)e^{\frac{j4\pi}{3}}\right] = I_i e^{j(\omega_i t - \emptyset_i)} \quad (5)$$

Respectively, where $\emptyset_o$ is the lagging phase angle of the output current to the output voltage and $\emptyset_i$ is that of the input current to the input voltage.

A. Switching Principle

The three phase matrix converter (MC) topology is shown in Figure 1.

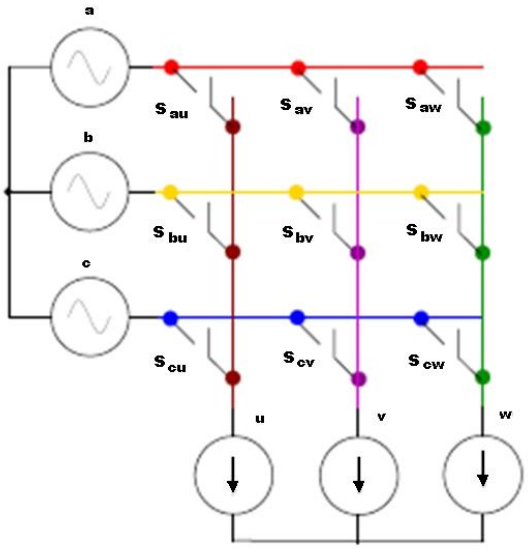

Figure 1**:** Three phase matrix converter

Since MC connects load directly to the voltage source by using nine bidirectional switches, the input phases must never be shorted, and due to the inductive nature of the load, the output phases must not be left open. If the switching function of a switch, S_{ij} in Figure 1, is defined as

$$S_{ij} = \begin{cases} 1, & S_{ij}\ close \\ 0, & S_{ij}\ open \end{cases} \quad i \in \{u, v, w\}, j \in \{a, b, c\} \quad (6)$$

The constraints can be expressed as

$$S_{ia} + S_{ib} + S_{ic} = 1, \quad (7)$$

For a three phase MC there are 27 valid switch combinations giving thus 27 voltage vectors as shown in Table 1. The switching combinations can be classified into three groups which are, synchronously rotating vectors, stationary vectors and zero vectors.

Table 1: Matrix converter switching vectors

Group	ON Switch			V_u	V_v	V_w	I_a	I_b	I_c	V_O	ω_O	I_i	ω_i
I	S_{au}	S_{bv}	S_{bw}	V_a	0	$-V_a$	I_u	$-I_u$	0	$2/3V_a$	0	$2/\sqrt{3i_u}$	$-\pi/6$
	S_{bu}	S_{av}	S_{aw}	$-V_a$	0	V_a	$-I_u$	I_u	0	$-2/3V_a$	0	$-2/\sqrt{3i_u}$	$-\pi/6$
	S_{bu}	S_{cv}	S_{cw}	V_b	0	$-V_b$	0	I_u	$-I_u$	$2/3V_b$	0	$2/\sqrt{3i_u}$	$\pi/2$
	S_{cu}	S_{bv}	S_{bw}	$-V_b$	0	V_b	0	$-I_u$	I_u	$-2/3V_b$	0	$-2/\sqrt{3i_u}$	$\pi/2$
	S_{cu}	S_{av}	S_{aw}	V_c	0	$-V_c$	$-I_u$	0	I_u	$2/3V_c$	0	$2/\sqrt{3i_u}$	$7\pi/6$
	S_{au}	S_{cv}	S_{cw}	$-V_c$	0	V_c	I_u	0	$-I_u$	$-2/3V_c$	0	$-2/\sqrt{3i_u}$	$7\pi/6$
	S_{bu}	S_{av}	S_{bw}	$-V_a$	V_a	0	I_v	$-I_v$	0	$2/3V_a$	$2\pi/3$	$2/\sqrt{3i_v}$	$-\pi/6$
	S_{au}	S_{bv}	S_{aw}	V_a	$-V_a$	0	$-I_v$	I_v	0	$-2/3V_a$	$2\pi/3$	$-2/\sqrt{3i_v}$	$-\pi/6$
	S_{cu}	S_{bv}	S_{cw}	$-V_b$	V_b	0	0	I_v	$-I_v$	$2/3V_b$	$2\pi/3$	$2/\sqrt{3i_v}$	$\pi/2$
	S_{bu}	S_{cv}	S_{bw}	V_b	$-V_b$	0	0	$-I_v$	I_v	$-2/3V_b$	$2\pi/3$	$-2/\sqrt{3i_v}$	$\pi/2$
	S_{au}	S_{cv}	S_{aw}	$-V_c$	V_c	0	$-I_v$	0	I_v	$2/3V_c$	$2\pi/3$	$2/\sqrt{3i_v}$	$7\pi/6$
	S_{cu}	S_{av}	S_{cw}	V_c	$-V_c$	0	I_v	0	$-I_v$	$-2/3V_c$	$2\pi/3$	$-2/\sqrt{3i_v}$	$7\pi/6$
	S_{bu}	S_{bv}	S_{aw}	0	$-V_a$	V_a	I_w	$-I_w$	0	$2/3V_a$	$4\pi/3$	$2/\sqrt{3i_w}$	$-\pi/6$
	S_{au}	S_{av}	S_{bw}	0	V_a	$-V_a$	$-I_w$	I_w	0	$-2/3V_a$	$4\pi/3$	$-2/\sqrt{3i_w}$	$-\pi/6$
	S_{cu}	S_{cv}	S_{bw}	0	$-V_b$	V_b	0	I_w	$-I_w$	$2/3V_b$	$4\pi/3$	$2/\sqrt{3i_w}$	$\pi/2$
	S_{bu}	S_{bv}	S_{cw}	0	V_b	$-V_b$	0	$-I_w$	I_w	$-2/3V_b$	$4\pi/3$	$-2/\sqrt{3i_w}$	$\pi/2$
	S_{au}	S_{av}	S_{cw}	0	$-V_c$	V_c	$-I_w$	0	I_w	$2/3V_c$	$4\pi/3$	$2/\sqrt{3i_w}$	$7\pi/6$
	S_{cu}	S_{cv}	S_{aw}	0	V_c	$-V_c$	I_w	0	$-I_w$	$-2/3V_c$	$4\pi/3$	$-2/\sqrt{3i_w}$	$7\pi/6$
II	S_{au}	S_{av}	S_{aw}	0	0	0	0	0	0	0	-	0	-
	S_{bu}	S_{bv}	S_{bw}	0	0	0	0	0	0	0	-	0	-
	S_{cu}	S_{cv}	S_{cw}	0	0	0	0	0	0	0	-	0	-
III	S_{au}	S_{bv}	S_{cw}	V_a	V_b	V_c	I_u	I_v	I_w	V_i	$\omega_i t$	i_O	$\omega_O t$
	S_{au}	S_{cv}	S_{bw}	$-V_c$	$-V_b$	$-V_a$	I_u	I_w	I_v	$-V_i$	$-\omega_i t + 4\pi/3$	i_O	$-\omega_O t$
	S_{bu}	S_{cv}	S_{aw}	$-V_{ab}$	$-V_{ca}$	$-V_{bc}$	I_v	I_u	I_w	$-V_i$	$-\omega_i t$	i_O	$-\omega_O t + 2\pi/3$
	S_{bu}	S_{av}	S_{cw}	V_b	V_c	V_a	I_w	I_u	I_v	V_i	$\omega_i t + 4\pi/3$	i_O	$\omega_O t + 2\pi/3$
	S_{cu}	S_{av}	S_{bw}	V_c	V_a	V_b	I_v	I_w	I_u	V_i	$\omega_i t + 2\pi/3$	i_O	$\omega_O t + 4\pi/3$
	S_{cu}	S_{bv}	S_{aw}	$-V_b$	$-V_a$	$-V_c$	I_w	I_v	I_u	$-V_i$	$-\omega_i t + 2\pi/3$	i_O	$-\omega_O t + 4\pi/3$

3. CONTROL ALGORITHM

The indirect transfer function approach is employed in both voltage source rectifier (VSR) and voltage source inverter (VSI) parts of the MC. Consider the VSR part of the circuit in Figure 2 as a standalone VSR loaded by a dc current generator, i_{dc}.

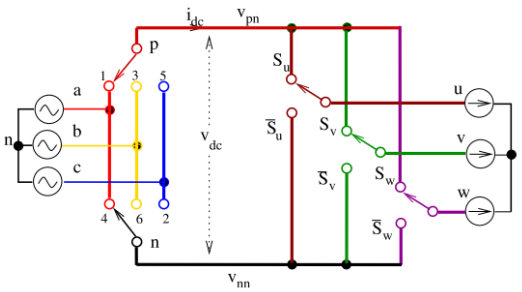

Figure 2: Indirect matrix conversion

A. Voltage Source Rectifier Space Vector Modulation

The VSR input current vector diagram is shown in Figure 3. The space vector of the desired input current can be approximated by two adjacent as shown in Figure 4. The duty cycles for VSR are calculated as (8)-(10).

$$\boldsymbol{d_{\alpha i} = m_i \cdot \sin\left(\frac{\pi}{3} - \theta_i\right)} \quad (8)$$

$$\boldsymbol{d_{\beta i} = m_i \cdot \sin\theta_i} \quad (9)$$

$$\boldsymbol{d_{0i} = 1 - d_{\alpha i} - d_{\beta i}} \quad (10)$$

Where m_i is the VSR modulation index

$$\boldsymbol{0 \le m_i \le 1} \quad (11)$$

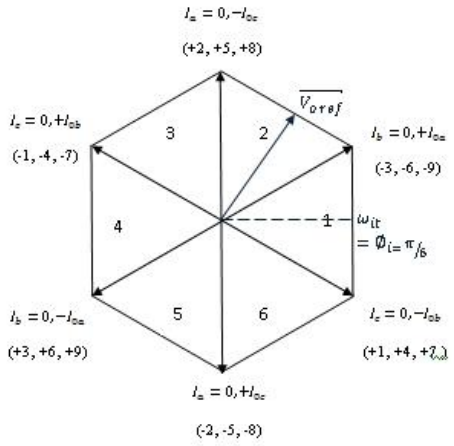

Figure 3: Input current vector diagram

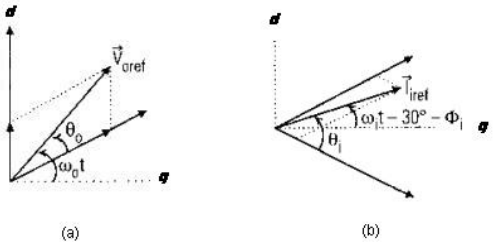

Figure 4: Vector diagrams (a) output sextant 2 (b) input sextant 1

For a switching cycle within the first sector

$$\begin{bmatrix}\vec{\imath}_a\\ \vec{\imath}_b\\ \vec{\imath}_c\end{bmatrix} = \begin{bmatrix}d_{\alpha i} + d_{\beta i}\\ -d_{\alpha i}\\ -d_{\beta i}\end{bmatrix} . I_{dc}$$

$$= \boldsymbol{m_i} \cdot \begin{bmatrix}\boldsymbol{\cos\left(\theta_i - \frac{\pi}{6}\right)}\\ \boldsymbol{-\sin\left(\frac{\pi}{3} - \theta_i\right)}\\ \boldsymbol{-\sin(\theta_i)}\end{bmatrix} . \boldsymbol{I_{dc}} \quad (12)$$

Substitute θ_i with

$$\boldsymbol{\theta_i = (\omega_i t - \varphi_i) + \frac{\pi}{6},\ \frac{\pi}{6} \le \omega_i t - \varphi_i \le -\frac{\pi}{6}} \quad (13)$$

φ_i is the arbitrary angle. The transfer matrix of the VSR, $\overline{T}_{VSR}$ is defined as

$$\begin{bmatrix}\vec{\imath}_a\\ \vec{\imath}_b\\ \vec{\imath}_c\end{bmatrix} = \boldsymbol{m_i} . \begin{bmatrix}\boldsymbol{\cos(\omega_i t - \varphi_i)}\\ \boldsymbol{\cos\left(\omega_i t - \varphi_i - \frac{2\pi}{3}\right)}\\ \boldsymbol{\cos\left(\omega_i t - \varphi_i + \frac{2\pi}{3}\right)}\end{bmatrix} . \boldsymbol{I_{dc}} = \boldsymbol{\overline{T}_{VSR} . I_{dc}} \quad (14)$$

Replacing the modulation index from (11) in (14) resulting the desired input current phase. The VSR output voltage is determined as

$$\bar{V}_{pn} = \bar{T}^T_{VSR} . V_{iph}$$

$$= \boldsymbol{\frac{3}{2} . m_i . V_{im} . \cos\varphi_i = constant} \quad (15)$$

B. Voltage Space Inverter Space Vector Modulation

Consider the VSI part of the MC in Figure 2 as a standalone VSI supplied by a dc voltage source $V_{pn} = V_{dc}$. The VSI switches can assume only six allowed combinations which yield nonzero output voltages. Hence, the resulting output line voltage space vector is defined by equation (2) can assume only seven discrete values, $V_0 - V_6$ in Figure 5, known as voltage switching state vectors.

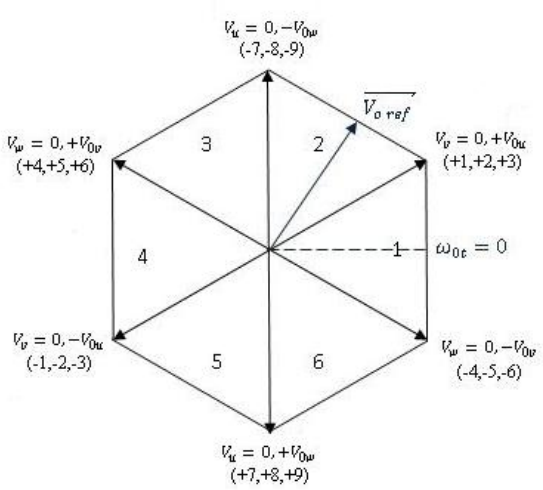

Figure 5: Output voltage vector diagram

The space vector of the desired output line voltages is

$$\bar{V}_o = \sqrt{3}\,.V_{oi}.e^{j(\omega_o t-\varphi\ +30^\circ)} \qquad (16)$$

$V_{oi}\ ; i \in \{u,v,w\}$.

can be approximated by two adjacent state vectors V_d and V_q, and the zero voltage vector, V_0 using PWM as shown in Figure 4, where $\bar{V}_{o\_ref}$ is the sampled value of $\bar{V}_o$ at an instant within the switching cycle T_s. The duty cycles of the switching state vectors are

$$d_{\alpha v} = m_v\,.\sin\left(\frac{\pi}{3} - \theta_v\right) \qquad (17)$$

$$d_{\beta v} = m_v\,.\sin\theta_v \qquad (18)$$

$$d_{0v} = 1 - d_{\alpha v} - d_{\beta v} \qquad (19)$$

where m_v is the VSI modulation index

$$0 \le m_v = \frac{(\sqrt{3}.V_{oi})}{V_{dc}} \le 1 \qquad (20)$$

The sectors of the VSI voltage vector diagram in Figure 5 correspond directly to the six sextants of the three phase output line voltages shown in Figure 6.

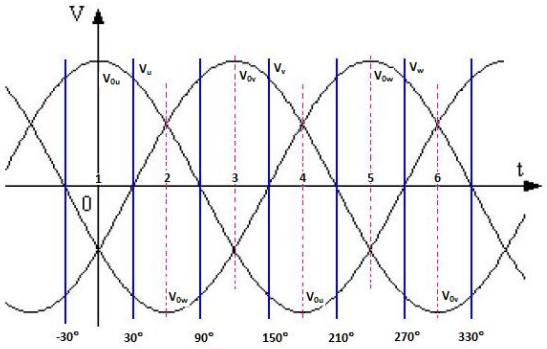

Figure 6: Six sextants of the output line voltage waveforms

The averaged output line voltages are

$$\begin{bmatrix}\vec{V}_u\\ \vec{V}_v\\ \vec{V}_w\end{bmatrix} = \begin{bmatrix} d_{\alpha v} + d_{\beta v}\\ -d_{\alpha v}\\ -d_{\beta v}\end{bmatrix}.V_{dc}$$

$$= m_v \cdot \begin{bmatrix}\cos\left(\theta_v - \frac{\pi}{6}\right)\\ -\sin\left(\frac{\pi}{3} - \theta_v\right)\\ -\sin(\theta_v)\end{bmatrix}.V_{dc} \qquad (21)$$

For the first sextant,

$$-30^\circ \le \omega_o t - \varphi_o + 30^\circ \le +30^\circ$$

and

$$\theta_v = (\omega_o t - \varphi_o + 30^\circ) + 30^\circ \qquad (22)$$

By substitution of (22) in (21)

$$\begin{bmatrix}\vec{V}_u\\ \vec{V}_v\\ \vec{V}_w\end{bmatrix} = m_v \cdot \begin{bmatrix}\cos(\omega_o t - \varphi_o + 30^\circ)\\ \cos(\omega_o t - \varphi_o + 30^\circ - 120^\circ)\\ \cos(\omega_o t - \varphi_o + 30^\circ + 120^\circ)\end{bmatrix}.V_{dc}$$

$$= \bar{T}_{VSI}\,.V_{dc} \qquad (23)$$

Substituting the modulation index from (20) in (23), the output line voltages are obtained

$$V_o = \begin{bmatrix}\vec{V}_u\\ \vec{V}_v\\ \vec{V}_w\end{bmatrix} = \sqrt{3}\,.V_{oi}\cdot\begin{bmatrix}\cos(\omega_o t - \varphi_o + 30^\circ)\\ \cos(\omega_o t - \varphi_o + 30^\circ - 120^\circ)\\ \cos(\omega_o t - \varphi_o + 30^\circ + 120^\circ)\end{bmatrix} \qquad (24)$$

The VSI averaged input current is determined as

$$\bar{\imath}_p = \bar{T}^T_{VSI}.i_o = \frac{\sqrt{3}}{2}\,.I_{om}\,.m_v.\cos(\varphi_L) = constant \qquad (25)$$

C. Output Voltage and Input Current SVM

Direct converter modulation can be derived from the indirect transfer function. First modulation is carried out as if the converter is an indirect. The switch control signals for DMC are then derived based on the relation between the VSR and VSI. The modulation index of the DMC is given as

$$\boldsymbol{m} = \boldsymbol{m_i}.\boldsymbol{m_v} \quad (26)$$

For simplicity, $m_v = 1$ and $m = m_i$.The modulation algorithm is derived similar to VSR and VSI except in the opposite direction. Since, both the VSR and VSI hexagons contain six sextants; there are 36 combinations or operating modes. However, only 27 valid switch combinations giving thus 27 voltage vectors as shown in Table 1. If the first output voltage and the first input current are active, the transfer matrix become

$$\bar{\boldsymbol{T}}_{\boldsymbol{ph}} = \boldsymbol{m}.\begin{bmatrix} \cos\left(\theta_v - \frac{\pi}{6}\right) \\ -\sin\left(\frac{\pi}{3} - \theta_v\right) \\ -\sin(\theta_v) \end{bmatrix} \cdot \begin{bmatrix} \cos\left(\theta_i - \frac{\pi}{6}\right) \\ -\sin\left(\frac{\pi}{3} - \theta_i\right) \\ -\sin(\theta_i) \end{bmatrix}^T \quad (27)$$

The output line voltages are

$$\boldsymbol{V_o} = \begin{bmatrix} \vec{V}_u \\ \vec{V}_v \\ \vec{V}_w \end{bmatrix} = \begin{bmatrix} d_{\alpha v} + d_{\beta v} \\ -d_{\alpha v} \\ -d_{\beta v} \end{bmatrix}.\begin{bmatrix} d_{\alpha i} + d_{\beta i} \\ -d_{\alpha i} \\ -d_{\beta i} \end{bmatrix}^T.\begin{bmatrix} V_a \\ V_b \\ V_c \end{bmatrix} \quad (28)$$

$$\boldsymbol{V_{ab}} = \boldsymbol{V_{a0}} - \boldsymbol{V_{b0}} \ \boldsymbol{and} \ \boldsymbol{V_{ac}} = \boldsymbol{V_{a0}} - \boldsymbol{V_{c0}} \quad (29)$$

which finally yield to

$$\begin{bmatrix} \vec{V}_u \\ \vec{V}_v \\ \vec{V}_w \end{bmatrix} = \begin{bmatrix} d_{\alpha\_vi} + d_{\beta\alpha\_vi} \\ -d_{\alpha\_vi} \\ -d_{\beta\alpha\_vi} \end{bmatrix}.V_{ab} + \begin{bmatrix} d_{\alpha\beta\_vi} + d_{\beta\_vi} \\ -d_{\alpha\beta\_vi} \\ -d_{\beta\_vi} \end{bmatrix}.V_{ac} \quad (30)$$

Where,

$$d_{\alpha\_vi} = d_{\alpha_v}.d_{\alpha_i} = m.\sin\left(\frac{\pi}{3} - \theta_v\right).\sin\left(\frac{\pi}{3} - \theta_i\right) = \frac{T_{\alpha\_vi}}{T_s}$$

$$\boldsymbol{d_{\beta\alpha\_vi}} = d_{\beta_v}.d_{\alpha_i} = m.\sin(\theta_v).\sin\left(\frac{\pi}{3} - \theta_i\right) = \frac{T_{\beta\alpha\_vi}}{T_s}$$

$$\boldsymbol{d_{\alpha\beta\_vi}} = \boldsymbol{d_{\alpha_v}}.\boldsymbol{d_{\beta_i}} = \boldsymbol{m}.\boldsymbol{\sin\left(\frac{\pi}{3} - \theta_v\right)}.\boldsymbol{\sin(\theta_i)} = \frac{\boldsymbol{T_{\alpha\beta\_vi}}}{\boldsymbol{T_s}}$$

$$d_{\beta\_vi} = d_{\beta_v}.d_{\beta_i} = m.\sin(\theta_v).\sin(\theta_i) = \frac{T_{\beta\_vi}}{T_s}$$

(31)

As can be seen, the output line voltages are synthesized inside each switching cycle from samples of two input line voltages, $\boldsymbol{V_{ab}}$ and $\boldsymbol{V_{ac}}$.
By comparison of (30) and (31), it can be concluded that simultaneous output voltage and input current SVM can be obtained by employing the standard VSI SVM sequentially in two VSI sub topologies of the three phase MC.

When the standard VSI SVM is applied in the first VSI sub topology, where $V_{pn} = V_{ab}$, the duty cycles of the two adjacent voltage switching state vectors are d_{α_vi} and $d_{\beta\alpha\_vi}$ as defined in (31). The standard VSI SVM in the second sub topology, with $V_{pn} = V_{ac}$, results in the state switching vector duty cycles $\boldsymbol{d_{\alpha\beta\_vi}}$ and $\boldsymbol{d_{\beta\_vi}}$, also defined as (31). The remaining part of the switching cycle is given as

$$\boldsymbol{d_0} = \boldsymbol{1} - \boldsymbol{d_{\alpha\_vi}} - \boldsymbol{d_{\beta\alpha\_vi}} - \boldsymbol{d_{\alpha\beta\_vi}} - \boldsymbol{d_{\beta\_vi}} \quad (32)$$

4. MATHEMATICAL MODELING

The complete model of MC is shown in Figure 7. It comprises input modulator, output modulator, MC modulator and MC IGBTs switches.

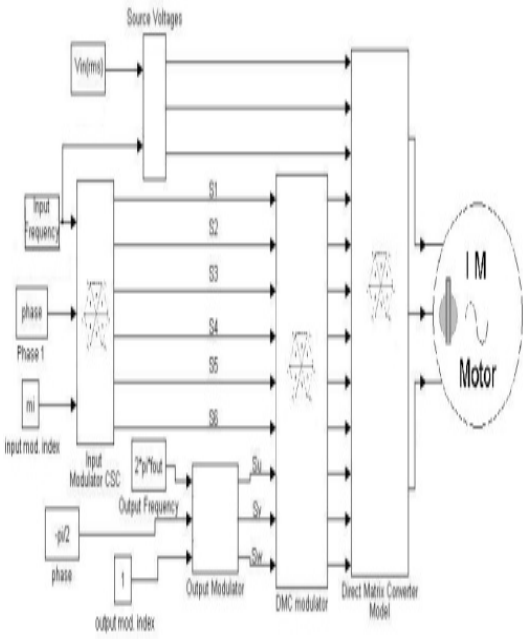

Figure 7: Block diagram of simulation model for direct matrix converter

Figure 8 is the sector identification and reference angle generation. The angle is generated from the reference output frequency by integrating it. Based on the angle, the sector can be identified. The result is shown in Figure 11. The modulation of input current is shown in Figure 9; the output voltage modulation is similar to VSI. The switch control signals for MC are shown in Figure 10.

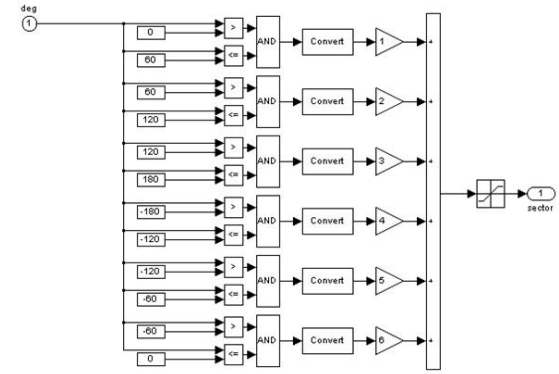

Figure 8: Sector identification

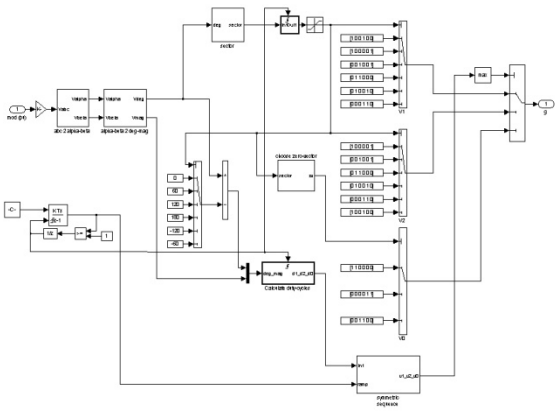

Figure 9: Input modulation

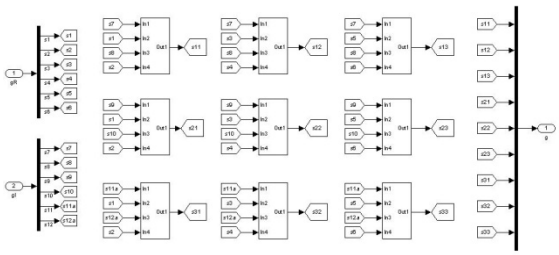

Figure 10: Direct matrix converter modulator

5. RESULT AND DISCUSSION

The simulations of direct matrix converter are carried out using MATLAB/SIMULINK. The processing took 56 seconds for the passive *RL* load and 45 seconds for the induction machine load. It was loaded by three phase induction motor (3hp, 200V, 60Hz star connected) for 0.5 and 0.866 transfer ratio.

Figure 12 shows the sector identification and reference angle generation. The angle is generated from the reference output frequency by integrating it. Based on the angle, the sector can be identified.

The input and output line voltage with loaded passive load is shown in Figure 13 and 14 for transfer ratio of 0.5 and 0.866. For the induction machine loaded the simulation result is shown in Figure 15 and 16. Figure 16 and 17 is the input current for the passive load and induction motor load respectively. The input currents are mostly sinusoidal for the induction motor load.

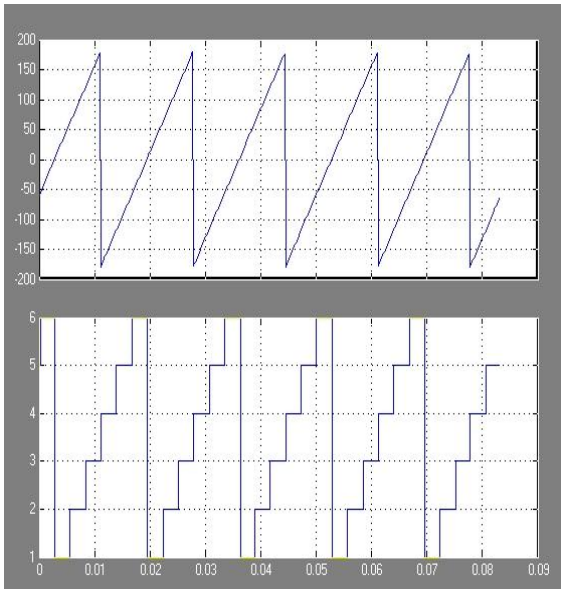

Figure 11: Result for sector identification

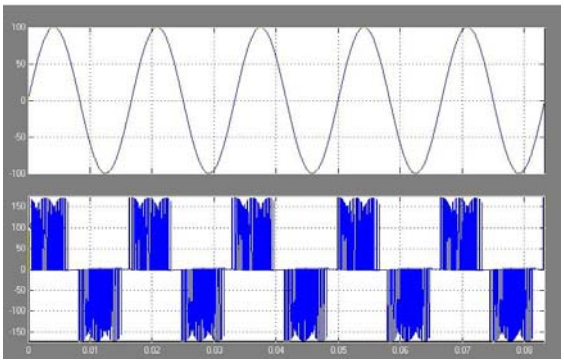

Figure 12: Input and output voltage with passive load for q=0.5; R=135.95Ω, L=168.15mH, V_{im}=100 V, f_o = 60Hz, f_s = 2kHz

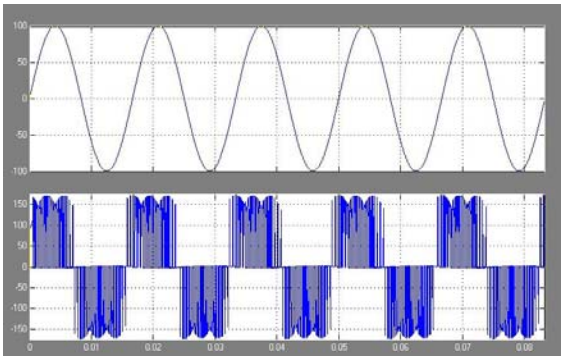

Figure 13: Input and output voltage with passive load for q=0.866; R=135.95Ω, L=168.15mH, V_{im}=100 V, f_o = 60Hz, f_s = 2kHz

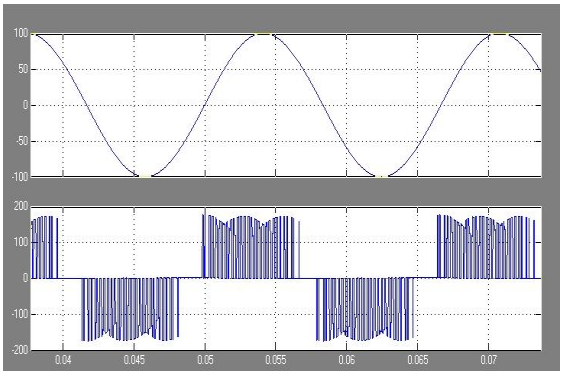

Figure 14: Input and output voltage with loaded induction motor for q=0.5; 3hp, R_s =0.277Ω, R_r=0.183Ω, N_r=1766.9rpm, L_m=0.0538H, L_r=0.05606H, L_s=0.0533H, f_o=60Hz, f_s=2kHz

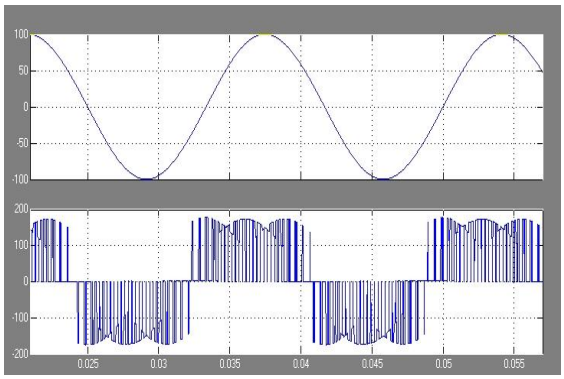

Figure 15: Input and output voltage with loaded induction motor for q=0.866; 3hp, R_s =0.277Ω, R_r=0.183Ω, N_r=1766.9rpm, L_m=0.0538H, L_r=0.05606H, L_s=0.0533H, f_o=60Hz, f_s=2kHz

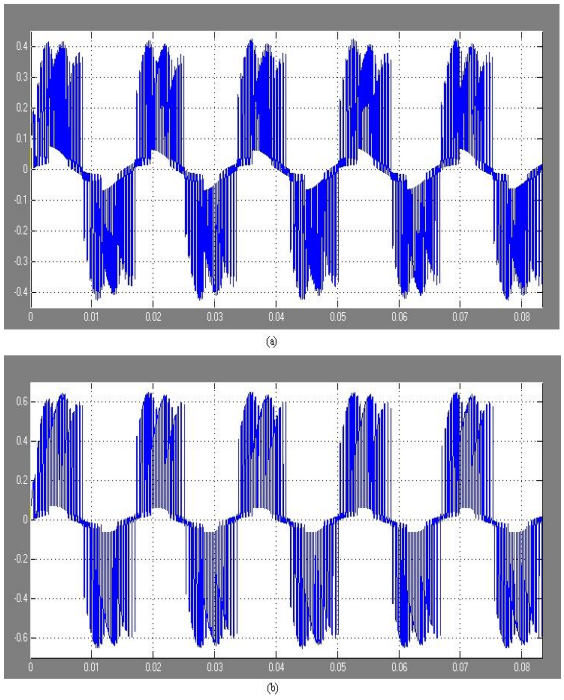

Figure 16: Input current with passive load; R=135.95Ω, L=168.15mH, V_{im}=100 V, f_o = 60Hz, f_s = 2kHz (a) q=0.5, (b) q = 0.866

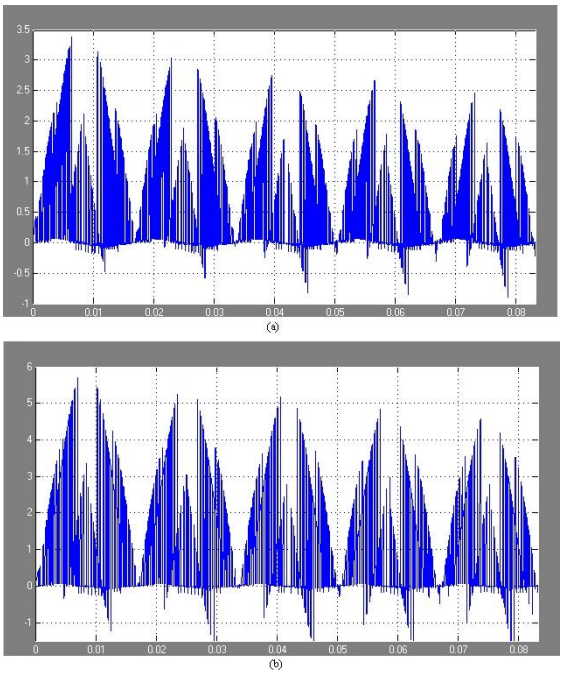

Figure 17: Input current with loaded induction motor for q=0.866; 3hp, R_s =0.277Ω, R_r=0.183Ω, N_r=1766.9rpm, L_m=0.0538H, L_r=0.05606H, L_s=0.0533H, f_o=60Hz, f_s=2kHz

6. CONCLUSION

The main constraint in the theoretical study of matrix converter control is the computation time it takes for the simulation. This constraint has been overcome by the mathematical model that resembles the operation of power conversion stage of matrix converter. This makes the future research on matrix converter easy and prosperous. The operation of direct control matrix converter was analysed using mathematical model with induction motor load for 0.866 voltage transfer ratio.

7. ACKNOWLEDGEMENT

The authors thank the Faculty of Electrical and Electronic Engineering of WHO that funded the project with resources received for research from both University of Malaysia Pahang and TATi University College (Short Grant 9001-9001).

REFERENCES:

[1]. A. Alesina, M.G.B.V., *Analysis And Design Of Optimum-Amplitude Nine – Switch Direct AC-AC Converters.* IEEE Trans. On Power. Electronic, 1989. 4.

[2]. D. Casadei, G.S., A. Tani, L. Zari, *Matrix Converters Modulation Strategies : A New General Approach Based On Space-Vector Representation Of The Switch State.* IEEE Trans. On Industrial Electronic, 2002. 49(2).

[3]. P. W. Wheeler, J.R., J. C. Claire, L. Empringham, A. Weinstein, *Matrix Converters : A Technology Review.* IEEE Trans. On Industrial Electronic, 2002. 49(2).

[4]. H. Hara, E.Y., M. Zenke, J.K. Kang, T. Kume. *An Improvement Of Output Voltage Control Performance For Low Voltage Region Of Matrix Converter*. In *Proc 2004 Japan Industry Applications Society Conference, No. 1-48, 2004. (In Japanese)*. 2004

[5]. Ito J, S.I., Ohgushi H, Sato K, Odaka A, Eguchi N., *A Control Method For Matrix Converter Based On Virtual Ac/Dc/Ac Conversion Using Carrier Comparison Method.* Trans Iee Japan Ia 2004. 124-D: P. 457–463.

[6]. Cha Hj, E.P., *An Approach To Reduce Common Mode Voltage In Matrix Converter*. Ieee Trans Ind Appl 2003. 39: P. 1151–1159

[7]. Helle L, L.K., Jorgensen Ah, Nielsen Sm, Blaabjerg F. , *Evaluation Of Modulation Schemes For Three-Phase Matrix Converters.* Ieee Trans Ind Electron 2004. 51: P. 158–171.

[8]. Huber L, B.D., *Space Vector Modulated Three Phase To Three Phase Matrix Converter With Input Power Factor Correction.* Ieee Trans Ind Appl, 1995. 31: P. 1234–1246.

[9]. Odaka A, S.I., Ohgushi H, Tamai Y, Mine H, Ito J. *A Pam Control Method For Matrix Converter*. In *Proc 2005 Japan Industry Applications Society Conference*. 2005